Multistate flow devices for geophysical fluid dynamics and climate

J. A. Whitehead[a)]
Department of Physical Oceanography, Woods Hole Oceanographic Institution, Woods Hole, Massachusetts 02543

W. Gregory Lawson
Department of Earth, Atmospheric, and Planetary Sciences, Massachusetts Institute of Technology, Cambridge, Massachusetts 02139

John Salzig
Department of Physical Oceanography, Woods Hole Oceanographic Institution, Woods Hole, Massachusetts 02543

(Received 26 January 2000; accepted 17 October 2000)

Two fluid devices exhibit simple aspects of nonlinear finite-amplitude instability in laminar fluid flow. The first shows multiequilibria; two steady flow regimes can be found within a certain range of the control parameter. The flow exhibits hysteresis as the control parameter is slowly increased and then decreased through this range of the control parameter. The second shows transition from steady flow to finite amplitude oscillations within a certain range. The two experiments share similar dynamics and only use different control parameters. A third experiment is described that exhibits either multiequilibria or oscillations, depending on which variable is selected to be the control parameter.
[DOI: 10.1119/1.1339278]

I. INTRODUCTION

A large number of nonlinear processes act to determine the state of the earth's climate. The possibilities of both large nonlinear oscillations and multiple equilibrium climates are suggested not only by data of past climates but also by models of climate. In the ocean a number of boundary effects produce the motion of the water, including wind stress, differential heating, precipitation, and evaporation. Internal factors such as radiant heating and tides also contribute. For over thirty years, it has been known that combinations of these forcing factors can produce a body with more than one steady and stable physical state. The first famous ocean example[1] involves the effects of the advection of temperature and salinity on a simple mixed basin that is connected to a second basin by two tubes, one over the other. In that problem, there were two stable fixed points and one unstable fixed point for some range of the forcing parameters. There have since been well over a dozen theoretical and modeling studies of such problems[2] usually with more complicated basins and more states. In addition, multiple equilibrium states have been predicted for forced convection[3] and in basins forced by surface stress alone.[4] These multiequilibrium problems contain more than one stable (locally) steady solution to the governing equations for identical boundary conditions. There are also oscillations possible for such problems. This is based on the behavior of both simple and complex ocean models in conjunction with some suggestive natural data.[5] In addition, there are a number of nonlinear oscillations associated with models of earthquakes,[6] glacial surges,[7] and volcanism.[8] These problems involve transition from one laminar flow to another. They differ from many of the common transition phenomena in fluid mechanics such as turbulence in fluids, as analyzed as finite amplitude stability phenomena,[9] because no wave numbers, eigenvalues, frequencies, or other internal degrees of freedom differentiate the two states as is the case for transition to more turbulent flow.

Such considerations have motivated us to seek physical examples using simple laboratory devices. Typical behavior has been found in some laboratory experiments[10,11] but these require elaborate facilities and very careful control of the driving parameters. The behavior is also indicated by some measurements of natural phenomena,[12] but firsthand data are again not readily available without large facilities. Of course, some electronic circuits and magnetic phenomena are well known to have the observed features,[13] and the mathematical concepts of their macroscopic properties are well developed.[14] In spite of this, here we present simple models utilizing fluid flow so that the parallels with the natural phenomena are visible and obvious. In this way, the devices are pedagogical for a wide range of students and scientists interested in natural phenomena. Naturally, these also illuminate the features of these problems in nonlinear multiple equilibria and oscillations in their own right.

II. MULTIPLE EQUILIBRIA

A simple box model of a wind and thermally driven ocean[3,11] is a fine example of multiple equilibria, in which more than one steady flow can exist for identical dynamics and boundary conditions. Consider a bay [Fig. 1(a)] connected to the ocean by a narrow deep passage. Let water in the ocean be directed toward the opening by a surface current driven by the wind. In the absence of density differences between ocean and bay water, the surface water flows into the bay, becomes mixed by winds and tides, and flows out below the inflow through the deep part of the passage. Also, let the bay water be heated. In that case, the warm bay water would tend to float outward through the gap at the surface and thus be directed against the wind-driven current. Two flow states are possible in a certain range of parameters. One of them is directed in the direction of the wind-driven current and the other is directed in the opposite direction.

The oceanic situation is similar to the case sketched in Fig. 1(b), where a vertical tube of height H is in a large basin of

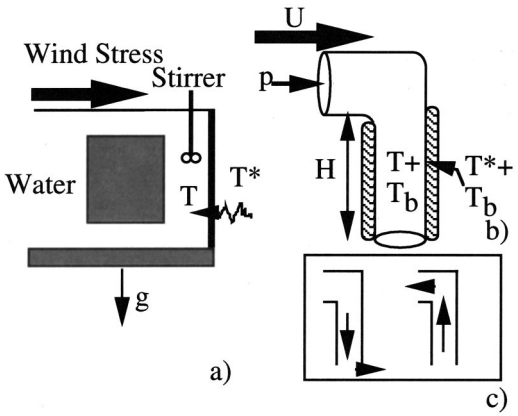

Fig. 1. Sketches of situations where heating and an incipient current produce multiple equilibria. (a) The ocean model (Refs. 3 and 11). A chamber representing a bay has temperature T in contact with a bath with temperature T^*. The bay is also subjected to wind stress that drives surface water into the surface of the bay. (b) A simple variation of the model. A current coming from the left impinges upon a submerged tube that has sidewall heating like the heating in the bay. The current produces a stagnation pressure p. (c) A sketch of the two flow states inside the tube. In the left flow state, the hot plume is driven down and out the bottom by the main current. In the right flow state, the hot plume rises up through the tube and creates a thermally driven flow directed against the main current.

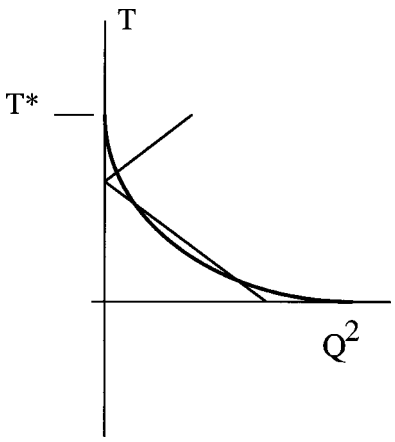

Fig. 2. Two sets of curves for the configuration sketched in Fig. 1(b). The straight lines are the solutions for Eqs. (2.4) and (2.5). The hyperbola is given by (2.7).

flowing water (which is a model of the ocean) with temperature T_b. The tube has an inlet at the top facing the direction of uniform flow of speed U. This flow provides positive, constant stagnation pressure ($=\frac{1}{2}\rho U^2$, where ρ is the density of the water in the basin). A second opening at the bottom allows outflow. The tube wall is in contact with a hot bath at temperature T^*+T_b. This resembles the problem of chimney ventilation on a windy day. Cold air can blow down the chimney, but if warm air ascends the chimney, a draft is produced which perpetuates the ascending flow. The dynamics of this configuration will be analyzed using simple approximations to the dynamics. Let us assume that heat conducts through the wall and brings water in the tube to temperature $T+T_b$. A dynamic equation is obtained using Bernoulli's equation (essentially conservation of energy[15]). Because this applies to steady frictionless flow Bernoulli's equation is also found to hold along streamlines in the momentum equation.[16] The equation holds in a number of regions that will be connected together. First, the equation holds in a region between upstream and the top inlet to the tube in the form

$$\rho(\tfrac{1}{2}U^2+gz_{\text{top}})+p_{\text{topE}}=\rho(\tfrac{1}{2}w^2+gz_{\text{top}})+p_{\text{topI}}. \tag{2.1}$$

Vertical velocity inside the tube w is positive upward, z is the vertical location, p is pressure, and g is acceleration due to gravity. The subscript top refers to the elevation of the streamline at the middle of the top inlet; bottom refers to the elevation at the bottom inlet; and the designation E or I refers to external or internal to the tube. We assume that the fluid temperature jumps up inside the tube to the value $T+T_b$. Bernoulli's equation along a vertical streamline inside the tube is $\frac{1}{2}\rho(1-\alpha T)w^2+\rho(1-\alpha T)z_{\text{top}}+p_{\text{topI}}=\frac{1}{2}\rho(1-\alpha T)w^2+\rho(1-\alpha T)z_{\text{bottom}}+p_{\text{bottomI}}$, where α is coefficient of thermal expansion. This reduces to

$$p_{\text{bottomI}}-p_{\text{topI}}=\rho(1-\alpha T)gH, \tag{2.2}$$

where $H=(z_{\text{top}}-z_{\text{bottom}})$. Bernoulli's equation in the outer fluid is $\rho(\frac{1}{2}U^2+gz_{\text{top}})+p_{\text{topE}}=\rho(\frac{1}{2}U^2+gz_{\text{bottom}})+p_{\text{bottomE}}$. This reduces to

$$p_{\text{bottomE}}-p_{\text{topE}}=\rho gH. \tag{2.3}$$

Setting $p_{\text{bottomI}}=p_{\text{bottomE}}$ and using (2.1)–(2.3) gives the following equation for vertical velocity within the tube:

$$w=\text{sgn}(2g\alpha TH-U^2)\sqrt{|U^2-2g\alpha TH|}. \tag{2.4}$$

This can be considered a modified version of Torricelli's theorem for a fluid in a field of gravity with internal changes in density. The substitution of density variation in the gravitational force term and nowhere else is often used in geophysical fluid dynamics. It is frequently used in the differential equations of momentum. The Boussinesq approximation defines the broad range of conditions under which this approximation is valid. The volume flux out of the tube of radius R is

$$Q=\pi R^2 w. \tag{2.5}$$

The relation between Q^2 and T from (2.4) and (2.5) is shown as the two straight lines in Fig. 2.

The heat balance in the container is simple relaxation-advection

$$\frac{\partial T}{\partial t}=\frac{1}{\tau}[T^*-T]-\frac{|Q|T}{V}, \tag{2.6}$$

where volume in the vertical portion of the tube is $V=\pi R^2 H$ and τ is the time constant for a change of temperature of water in the tube. The time constant might arise from diffusion of heat through the walls and into the interior of the fluid. For steady state

$$T=\frac{T^*}{1+\dfrac{|Q|\tau}{V}}, \tag{2.7}$$

which defines the hyperbola shown in Fig. 2. The two straight lines intersect the hyperbola in three places. The bottom and top intersection points are stable solutions. The middle is unstable[1] and the system evolves to either one of the two stable states. In addition to ocean or geophysical situations, ventilation in such settings as smokestacks, fur-

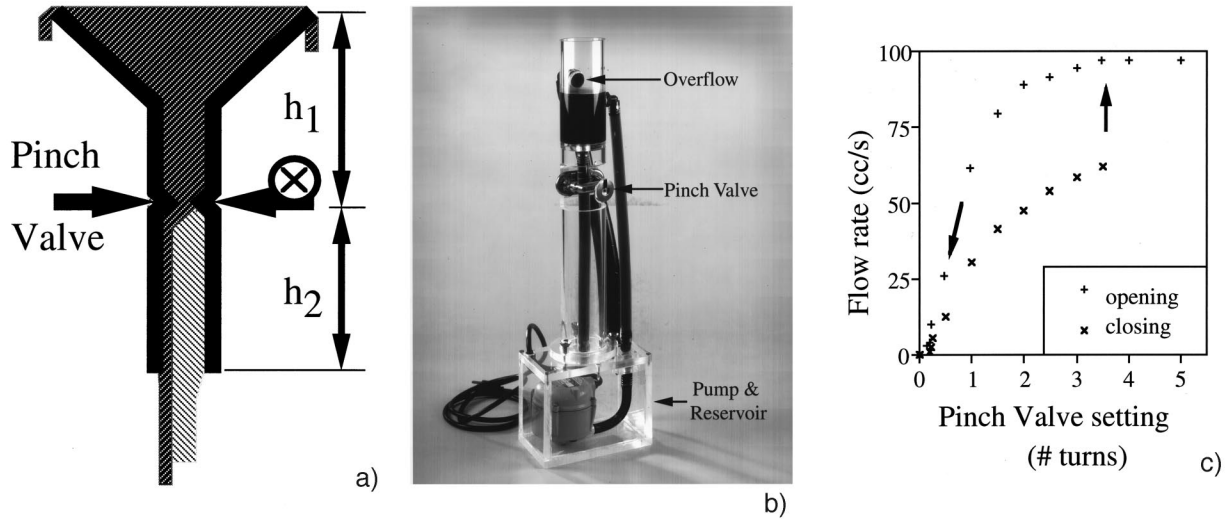

Fig. 3. (a) A pinched tube holding water coming from an overflowing funnel demonstrates multiple states within a parameter range. One state has the air–water interface separate below the pinch (dark hatched region). In the second, water fills the tube to the bottom (this includes both dark and light hatched regions). (b) Photograph of the portable classroom demonstration apparatus. (c) Measurements of flow rate in an experiment where the valve was turned slowly and the flow then came to a new steady equilibrium. The arrows show the direction of adjustment.

naces, ships, fires, rooms, mines, and skyscrapers in suitable winds or with some blowers might have two such flow states, one driven mostly by temperature and the other driven by the winds or blowers. One of the states might be undesirable or dangerous.

A demonstration device for multiple equilibria. A simple laboratory water device which shows this kind of multiple equilibrium is schematically sketched in Fig. 3(a). In this device, air is used instead of temperature to produce a buoyancy force. A funnel is fitted into a piece of transparent tubing that has a variable clamp midway along the tube. The funnel and tube must be firmly mounted with the funnel lying above the tube and with their central axis vertical. The funnel and tube must be placed in a location with a source of constant water flux and adequate water drainage such as a sink, or outdoors. Water should be steadily directed into the funnel at a rate great enough to overflow the funnel when the clamp is fully opened. Water will also descend through the tube. Assuming the greatest drag, and hence the greatest pressure drop, is across the pinch, pressure difference across the pinch comes from a positive pressure due to hydrostatic head from the water lying above the pinch (in the tube and funnel) minus a pressure below the pinch that is less than atmospheric from the siphon action of water in the tube below the pinch. If the clamp is wide open, the tube becomes completely filled with flowing water. If the clamp is partially closed, below a critical flow rate air travels up from the bottom of the tube to the pinch so that the siphon effect in the lower tube is lost. Driving pressure across the pinch is thereby reduced. This is fully visible in the transparent tubing. In the air-bound state, flow is considerably slower than when the bottom tube is filled with water. We will show below that the governing equations can have behavior similar to that sketched in Fig. 2.

Our device uses a 0.0125-m-diam, 0.28-m-long vertical, flexible, transparent, Tygon tube. The top of the tube is connected to the bottom of a vertical cylinder that has a 0.02-m-diam overflow tube in its sidewall. The cylinder substitutes for the funnel and serves as a reservoir whose water surface is kept at a constant level 0.1 m higher than the top of the Tygon tube. The adjustable pinch valve is placed 0.08 m below the floor of the cylinder so that $h_1 = 0.18\,\mathrm{m}$ and $h_2 = 0.2\,\mathrm{m}$ [these are defined in Fig. 3(a)]. A submersible pump is located in a catch basin below the tube and overflow tube. We have a portable classroom demonstration device [Fig. 3(b)] to show the desired processes. It consists of a pump and reservoir in a rectangular plastic container attached by quick release holders to a cylinder that holds the upper tube, the flexible tube, and the pinch valve. The overflow tube and the tube from the pump can be separated from the pump and reservoir so that the two parts can be taken apart and fit into a suitcase for travel. On our device, the overflow diameter has proven to be slightly too small to handle the overflow. If the flow rate through the tube is almost zero we have to slightly decrease the rate of the pump with a pinch valve (not shown) on the pump tube to avoid overflowing the top tube. The device has been taken on numerous trips and used in lectures to illustrate the multiple states that such climate-like devices can have.

Measurements of flow rate as a function of the number of valve turns reveal the features of interest as shown in Fig. 3(c). The top data were obtained as the valve was started fully open and then was gradually closed. At a value of about 0.2 turns from fully closed, the flow dropped to a lower level that corresponded to the lower tube suddenly becoming filled with air. The bottom data were obtained as the valve was opened between successive measurements. At a value of 3.5 turns, the flow at the base of the tube reached a value sufficient to drive air out of the bottom tube. The rate thereupon rose to a higher value which corresponded to the lower tube becoming flooded with water. Since the changes in valve setting were made very slowly, and the device was allowed to come to a steady state between each change, this device produces more than hysteresis (response lagging the change). It possesses two values of flow rate within a given range of valve settings as the valve is changed from fully open to fully closed and back to fully open. This also demonstrates the other typical features of multiple-equilibrium flows. The transition between the air-bound lower tube and the water-

filled lower tube is found at a very different valve opening as the valve is opened than as the valve is closed. In addition, the flow rate jumps from one value to another at transition.

The pressure difference across the valve during the flooded state can be thought of as being comparable to the constant wind pressure term in the above thermally driven problem. With the pinch valve fully open, water flows steadily down through the entire tube. We assume the formula for the velocity is like that in (2.4) with $T=0$. It stays steady since the pressure change across the valve stays constant. However, the area in (2.5) changes as the valve closes, so the flow rate (volume flux) goes down with area. As the flow rate is decreased by closing the valve, the air at the bottom outlet to the tube suddenly can force its way upward through the tube by buoyancy as the Froude number based on radius at the bottom of the tube falls below a critical value. The presence of air in the bottom tube can be thought of as temperature. The dynamics can be expressed by Eq. (2.4), but instead of Eq. (2.7) there is a step function relation between ''temperature'' (air content) and the flow. Above a critical flow rate the tube is filled with water and ''temperature'' (air content) is zero. At the critical flow rate, the air at the bottom of the tube creates a bubble whose rise speed equals the descent speed of the water. For lower flow rates, air rises up the lower part of the tube to the valve. Consequently, ''temperature'' (air content) jumps from zero to a fixed positive value for flow rates below this value. The diagram comparable to Fig. 2 is shown in Fig. 4, but the curves are inverted so that the pressure drop across the valve is plotted as a positive function of flow rate. Below the critical flow rate, the pressure, shown as a bold horizontal line, has a low constant value proportional to the pressure difference caused by the vertical distance from the top of the funnel to a spot immediately below the pinch where the air is encountered by the water. Above this critical rate, the aggregate pressure is also a horizontal bold line with a larger value proportional to the distance from top of the spillway to the bottom of the tube. The two are connected by a vertical curve.

The straight sloping lines describe the relationship between volume flux squared and pressure across the pinch for three different pinch valve settings. They are found using Eqs. (2.4) and (2.5) setting $\frac{1}{2}U^2=\rho g(h_1+h_2)$ and $\rho g\alpha TH=0$ or $-\rho gh_2$. One such solution is the light, solid, straight line shown in Fig. 4 that intersects the bold curve at three points. Two of the intersections are labeled ''2'' and ''4.'' We note first that if p_1 were larger in relation to p_1+p_2 as shown by the horizontally dashed bold line, intersection would only be at point 2. This could be produced, for example, by locating the value at lower elevation with everything else the same,

But instead of changing some geometric parameter, let us imagine that the valve has cross section of radius R that can be changed at will. We will imagine that R initially is set to a large value so the flow line is the dashed straight sloping line in Fig. 4. The rapidly flowing water fills the tube so that the flow is driven by pressure $p=p_1+p_2$ and the solution is the intersection near point 1. As we decrease R the straight line gets progressively steeper so solutions move along the upper curve toward the left, in the direction of the top arrow. As the dynamics curve enters the intermediate stage where one unstable and two stable values of intersection exist, the solution continues to move along the top curve, and reaches point 2. At the value where the top curve no longer intersects the dynamic curve for decreasing R, the air rises up the tube

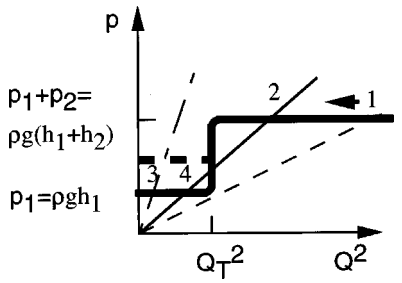

Fig. 4. A diagram comparable to Fig. 2 for the funnel experiment. The heavy solid curves give pressure produced by the static height of water in the cylinder and tube. Pressure p_1 is hydrostatic pressure due to water of depth h_1 (Fig. 3) and p_2 is hydrostatic pressure due to water of depth h_2. The heavy horizontal dashed line would replace the horizontal p_1 line for a valve located at lower elevations so that p_1 is greater. Consequently, p_2 is less by the same amount so the sum of pressures is the same. The light lines give laws for flow rate across the valve for three different settings. The value is increasingly open for smaller slopes. The symbol Q_T stands for the volume flux at transition.

so that ''temperature'' jumps up and the pressure changes to $p=p_1$. At this point, flow rate decreases, and only the lower intersection points are found as shown by point 3, which is the intersection of the heavy curve with the straight, light, long-and-short dashed line. This state continues as R goes to zero. Now let us imagine what happens as the valve is opened. For small R, volume flux through the tube is small compared to the flux at which the air bubble rose, so the water does not have sufficient flow rate to expunge the air from the lower part of the tube and ''temperature'' is high. Only the lower intersection point 3 exists. As radius R increases, the intermediate ''three-intersection'' stage is encountered, but the solution remains on a lower trajectory such as shown by point 4 since volume flux is below the critical value. At some value of R, the flow following the lower branch reaches the transition flow rate Q_T. Above this rate, intersection with the bottom curve terminates as air is driven from the lower part of the tube. As this happens, the flow rate jumps upward, reinforcing the elimination of air from the bottom portion of the tube. In the above analogy, ''temperature'' will plunge to zero as water is driven from the lower part of the tube. Upon the loss of air in the bottom part of the tube, flow rate will jump to a new higher value close to point 1. This high rate continues for all subsequent increases of R.

This kind of behavior is commonly found in chimneys that are poorly placed so that in the winter cold air is directed down the chimney by exterior winds. The unfortunate occupants find that a small fire results in the smoke being driven into the dwelling rather than up the flue when the chimney is cold. Only a large fire can overcome the downdraft sufficiently to force heat up the chimney walls and create an updraft. Fortunately, once heated the chimney can continue to serve with only a small fire.

III. A NONLINEAR OSCILLATOR

A small modification of the above device produces quite different behavior as sketched in Fig. 5. Assume now that a long, tall vertical cylinder replaces the funnel at the top, which had been overflowing. We bend the tube below the constriction upward and then downward again so there is a crest. This maximum in the tube height is at an elevation h_1

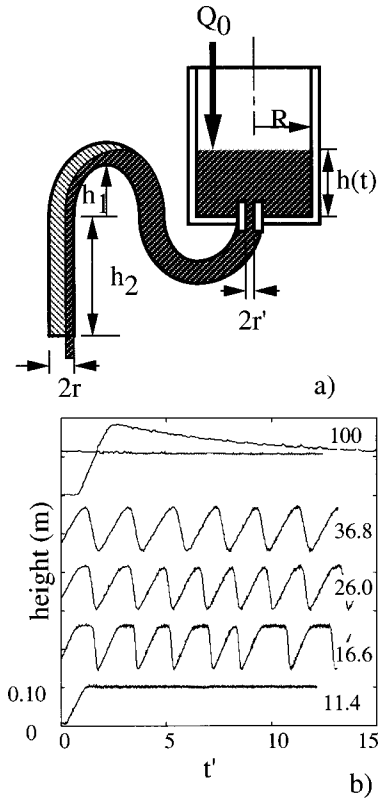

Fig. 5. (a) A device for producing oscillations with a critical flow and a siphon. (b) Height of water in the cylinder $h(t')$ for different values of input volume flux (the units are $10^{-6}\,\mathrm{m^3\,s^{-1}}$).

above the bottom of the cylinder. The bottom of the tube is located at a distance h_2 below the bottom of the cylinder. Water is fed into the cylinder at a constant rate Q_0, whereupon it flows out of the bottom through the tube. Imagine what happens for very slow flow, and in the absence of friction and with surface tension neglected. Water accumulates in the cylinder until the elevation of water in the cylinder exceeds the crest of the bend in the tube. The water in the tube then flows over the crest and becomes controlled at the topographic maximum (like flow over the weir of a dam). The free surface of the water lying above the tube crest adjusts itself so that the critically controlled flow matches the input. For increasing values of input the elevation of water in the cylinder and the elevation of the free surface in the tube increase. The contact point between air, water, and the top of the tube moves toward the crest of the top of the tube. At some specific value of input flow rate, depending mostly on the size of the tube, but also in reality on some aspects of tube shape and other physical properties such as surface tension and wettability of the tube material, the free surface contacts the crest of the top of the tube. Close to this stage, the steady flow develops instability and the behavior changes to that of a Tantalus cup,[17] which is a device in which a siphon is within a container with sides higher than the top of the siphon. The contact point at the top of the tube moves downstream, which causes pressure to drop at the crest of the tube so that pressure difference between the crest and the cylinder increases and flow rate in the tube increases. This drives the contact point further downstream within the tube, hence flow further accelerates. Quickly thereafter, the contact point is driven to the bottom of the tube, flow greatly increases, and the cylinder is emptied of water. At this stage, air enters the tube from upstream, the flow slows down or ceases, and the tube can no longer remove as much water as is being pumped in. Water level in the tube then builds up from zero again until the level reaches the crest. The cycle then repeats itself again and again.

We have conducted studies of flows in such a device with $R=0.032\,\mathrm{m}$, $h_1=0.118\,\mathrm{m}$, $h_2=0.64\,\mathrm{m}$, $r=0.0064\,\mathrm{m}$, and volume flux Q_0 set at values ranging up to $10^{-4}\,\mathrm{m^3\,s^{-1}}$. Figure 5 shows measurements of surface height, taken from pressure data, for a number of different values of input flow rate. Each curve is offset upward by 0.15 m. The numbers on the right correspond to the imposed volume flux. The time is divided by the time scale $\tau=\pi R^2 h_1/Q_0$. The bottom curve shows that for smaller volume flux the flow is steady. We saw visually that the flow becomes critically controlled at the crest of the tube. Water spilled out the rest of the way as sketched by the dark striped region in Fig. 5(a). For the next three volume fluxes upward, the flow oscillated. The oscillation sequence was as follows: After a height minimum, the cylinder would begin to fill and the water surface in the tube rose until the flow at the crest became critical. But then the free surface of the water intersected the top inner surface of the tube so that the air/water contact point moved down the tube. This drove air from the tube and produced a siphon that evacuated the cylinder and started the cycle again. We can estimate the critical volume flux, Q_{0c}, by assuming that the crest has a square cross section with sides of length r. We use the standard hydraulic formula for flow over a weir[18] of $Q=(2/3)^{3/2}gh_u^{3/2}r$ and set the fluid height at the crest $2/3h_u=r$. Thus $Q_{0c}=\sqrt{g}r^{5/2}=10.4\times10^{-6}\,\mathrm{m^3\,s^{-1}}$. This value is below the value of transition to oscillations seen in this experiment by about 50%. Since we only crudely approximated the geometric details, ignored surface tension effects, and simplified a number of other aspects of the real experiment, the experimental transition to oscillations could not be expected to happen exactly at the predicted value. Therefore, the agreement between the magnitude of Q_{0c} and the value of the experimental number for transition crudely supports this mechanism. For flows just above the critical value of volume flux, the oscillation amplitude is large. The actual instant when the emptying starts varies for each cycle and the flow is obviously not exactly periodic in the experiment. Theoretically, since there are only two time derivatives and the coefficients are constant, the equations would produce flows that approach either fixed points or periodic oscillations that correspond to limit cycles.[14]

For moderately greater values of volume flux, the oscillations become more regular. In dimensional time the cycle period decreases. This decrease is not very apparent using scaled time in Fig. 5(b), so the scaling parameter seems to roughly fit, but in real laboratory time the change in period with increasing pumping rate is obvious. The oscillations are saw-tooth alternations between filling and evacuation events. Above this is a range between the top two curves where a mixture of air and water enters the tube at irregular times and no cyclic flow is seen. But finally at flow rates great enough to support a steady siphon, the flow is steady again. The top curve shows such a steady flow being approached. For height starting from zero, the steady final value is overshot in order to prime the siphon, and then steady state is approached as a decaying curve. The assumption that the flow in the large tube is governed by Bernoulli's law, so that the criterion for

transition to steady flow is $\frac{1}{2}u^2 > gh_2$, produces an unrealistically great value of $Q_0 = 4.5\times10^{-4}\,\mathrm{m^3\,s^{-1}}$. Thus in our apparatus, we suspect that there is viscous drag along the tube walls.

Finally, experiments were done for assorted other values and signs of h_1 and h_2. For negative values of h_2 a range of multiple equilibria was found without oscillations similar to the experiments of Sec. II.

IV. THE ROLE OF THE CONTROL PARAMETER

Both problems have very similar features that can be understood by investigating the relation between the control parameter (independent variable) and the dependent variable for both the funnel and the siphon experiments. We will then show a ''unified diagram'' that has features of both of the above relations and describe an experiment that obeys this diagram. Thus, this final experiment possesses both the multiple equilibrium character of the funnel experiments and the oscillations of the siphon experiments, depending on which parameter we select to be the control parameter, or independent variable.

In the funnel experiment [Fig. 3(a)], we imagine that instead of a pinch valve there is a very small tube whose radius R (indicated as the ordinate) varies as the control parameter, and that (2.5) governs there. Thus we sketch in Fig. 6 that volume flux (the dependent variable given along the abscissa) goes as the square of radius R for fixed pressure drop $\rho g h_1$. A step increase in flux is found at a critical flux Q_1 where pressure changes abruptly to $\rho h(h_1+h_2)$. For this greater flux, a second curve also has volume flux proportional to the square of R. But this second curve is offset to the right because the bottom tube is filled with water and hence produces a siphon effect at those flow rates. Figure 6(a) shows the relations between flux and R^2 and this figure is similar to Fig. 3(c), but the axes are switched. The square of the pinch radius R is the control parameter, or independent variable, plotted along the abscissa in Fig. 6(a). Flow rate Q is the dependent variable, plotted as the ordinate in Fig. 6(a). As the control parameter is slowly changed, flow rate can take two values in a certain range.

For comparison, in the nonlinear oscillator volume flux Q_0 into the top of the tube is the control parameter. It is related to volume flux and height by volume conservation

$$A\frac{dh}{dt} = Q_0 - Q \tag{4.1}$$

for $h>0$. The volume flux in the tube obeys $Q = \pi g R^2\sqrt{g(h+h_2)}$ if the siphon is primed, and $Q = (2/3)^{3/2} g h_u^{3/2} R$ if the siphon is unprimed. This is plotted along the abscissa in Fig. 6(b), where in this case height h is the dependent variable given along the ordinate instead of R. The relations are thus somewhat similar to those in the funnel experiment although the equations are different in detail. More importantly, the behavior of the flow governed by the curves shown in Fig. 6(b) is similar to that of the curves in Fig. 6(a). If $Q_0 > Q_2$, a steady flow is found. In contrast, if $Q_1 < Q_0 < Q_2$, the flow out follows one of the two curves in Fig. 6(b). If the siphon is primed, then according to the curve on the right $Q > Q_0$ and Eq. (4.1) states that height h decays. Height reaches zero, then air is pulled into the tube and the flow out follows the curve on the left. Then Eq. (4.1) says that height h increases until the siphon is primed and the behavior jumps to the curve on the right again. At this time the flow out exceeds Q_0 and the cycle repeats itself. And finally, if $Q_0 < Q_1$ a steady flow is also found.

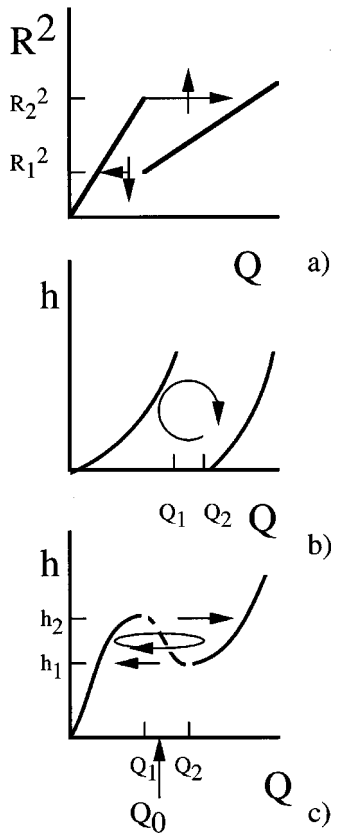

Fig. 6. Diagrams expressing the behavior of the two types of experiments. (a) Sketch of the solution to a simplified set of equations expressing the funnel experiment. The control parameter is R^2. If $R<R_1$, only the left-hand line is possible and so this gives the value of volume flux Q. If $R_1 < R < R_2$ either line is possible. If $R>R_2$, only the right-hand line is possible. As R is changed the solution can move along either line except if the line ends. In these cases, the arrows show transitions from one curve to the other. The vertical arrows show the direction of the change in R. The horizontal arrows show the direction of the consequential jump. (b) Sketch of solutions to a simplified set of equations to the siphon experiment. The control parameter is the steady forcing of volume flux Q_0. If $Q_0<Q_1$, only the left-hand curve gives the steady stable solution $Q=Q_0$. If $Q_1<Q_0 < Q_2$ no steady stable flow exists and oscillations are found. If $Q_0>Q_2$ the right-hand curve gives the steady solution $Q=Q_0$. (c) Sketch of solutions to a simplified set of equations for an experiment with a continuous curve. If h is the control parameter, the solutions exhibit multiple equilibrium features like the funnel experiment. If Q_0 is the control parameter the solutions exhibit the oscillatory features of the siphon experiment. A device that produces such a curve is shown in Fig. 7.

We also found that if negative values of h_2 were made impossible by elevating the bottom of the tube above the bottom of the cylinder in Fig. 5, steady multiple equilibria were found. This feature can be understood as an overlap of the two curves due to the fact that $Q_2<Q_1$.

An experiment that possesses a smooth curve and thus demonstrates both of the features, namely multiple equilibria and oscillations,[6,8] is also readily produced in the laboratory, but present models have response times of over an hour so that devices cannot quickly reveal the desired features. Its S-shaped curve relating h and Q is sketched schematically in Fig. 6(c). A diagram of the device[8] that produced it is sketched in Fig. 7. Corn syrup was fed into the top of a

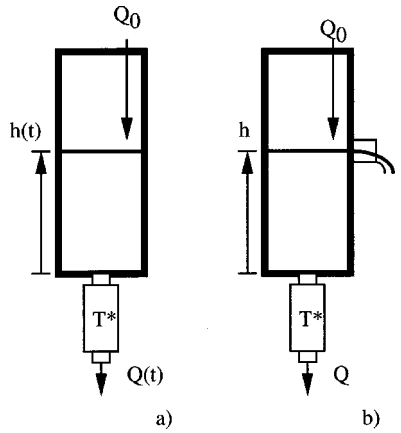

Fig. 7. (a) The apparatus with an input volume flux Q_0 of corn syrup as the control parameter. The corn syrup flows out through a chilled tube and a steady relation between pressure and flow rate obeys a curve as sketched in Fig. 6(c). For some parameters the height and flow rate oscillate with time. (b) The apparatus with an overflow that produces fluid height h as the control parameter. The flow (dependent variable) exhibits multiple equilibria like the funnel experiment.

vertical cylinder. This fluid has the property that the viscosity increases greatly as temperature is decreased, so the viscosity is about one order of magnitude greater when the syrup is about 15 °C colder. We used a gravity feed for the source Q_0 that consisted of a cylinder with a radius of about 0.1 m and with about 10-l capacity with a small tube 0.04 m in radius and 0.1 m long in the bottom. The cylinder that received this flow was 1 m high and 0.05 m diameter. At the bottom of this cylinder was an outflow that was fed out through a small copper tube 0.02 m in radius and 0.145 m long with about half its length immersed in antifreeze at roughly −11 °C. In this way, sufficiently slow flow in the copper tube caused the syrup to be very cold and thus very viscous. In contrast, fast flow allowed the syrup to transit the cooled regions quickly so that the syrup remained warm and it became only slightly more viscous. This device exhibited oscillations when fed by a steady flow of syrup into the top of the cylinder. In this demonstration device, oscillation periods were hours, and thus too long for classroom use unless students were free to leave it running and record the flows on time lapse video. Figure 7(b) shows a second configuration that produces multiple equilibria instead of oscillations. In this case the level of the syrup above the end of the copper tube is held constant in each run by a spillway. But the elevations of the spillway were varied from run to run. This is achieved in the laboratory by simply having a large holding tank for the syrup. In practice, the holding tank elevation above the bottom of the copper tube was the control parameter. It was simpler to vary the elevation of the copper tube and the sleeve around it with chilled antifreeze and keep the large holding tank fixed. Thus a wide flexible tube connected the holding tank and the chilled copper tube. As the elevation difference between the holding tank surface and the chilled tube outlet is slowly increased up from zero and then down again, flow follows the trajectory shown by the arrows in h,Q phase space in Fig. 6(c). This single apparatus thus exhibits all the features of the two preceding devices. However, it is very slow to cycle and typical cycle periods are over an hour. Thus unless this is automated, it does not allow convenient classroom study over an afternoon.

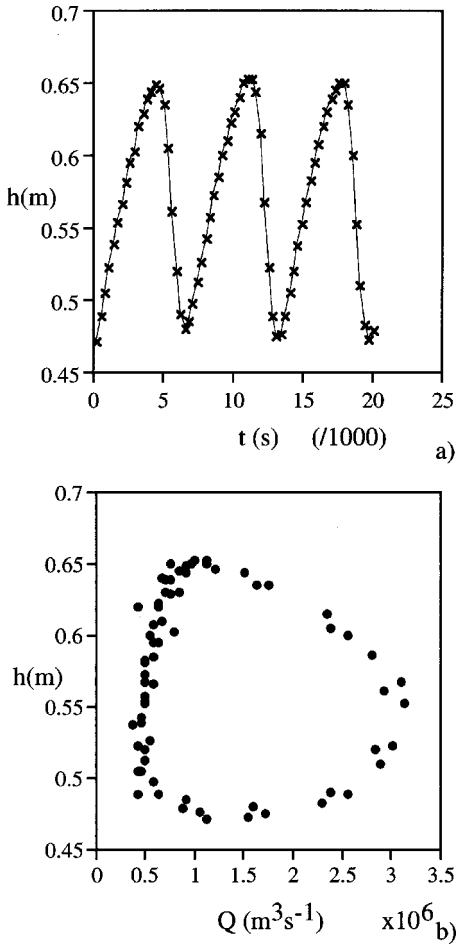

Fig. 8. Results of a laboratory experiment with a fluid that has a temperature-dependent viscosity. (a) Oscillations of height of the interface in the reservoir with time. (b) Phase plane of height and volume flux through the cooled tube as a function of time.

Naturally, to produce oscillations two time derivatives are needed. A typical set of complete oscillating model equations have the form[8]

$$\frac{\partial T}{\partial t}+Q\frac{\partial T}{\partial z}=-T, \quad T=1 \ \text{ on } \ z=0,$$

$$\mu(T)Q=-\frac{\partial p}{\partial z}, \quad p=0 \ \text{ at } \ z=1, \ p=P \ \text{ at } \ z=0, \qquad (4.2)$$

$$\epsilon\frac{\partial P}{\partial t}=Q_0-Q.$$

These equations are dimensionless. The depth of the cooled tube is the depth scale and the velocity scale is the depth scale divided by the thermal diffusion time scale. The first equation is conservation of heat with conduction between the fluid and the tube walls. This produces a relaxation time that generates the right-hand term of the top equation. The second equation is simple viscous flow. A likely equation for viscosity is $\mu_i(T)=e^{\beta(1-T)}$, which is an Arrhenius-type law with the denominator expanded as a Taylor series. The third represents pressure change from accumulation of material in a compressible reservoir. These particular equations are taken from a model that includes volatile effects on viscosity of magma during a volcanic eruption. The parameter T rep-

resents volatile content rather than temperature. Pressure of a compressible magma chamber is P. The right-hand term of the first equation arises from the time it takes volatile material to nucleate in bubbles. The equations are integrated in the vertical using a simple technique and then they were integrated in time numerically. As in our earlier examples of oscillating systems, Q_0 is the control parameter and oscillations are found for a fixed range of Q_0.[8] If the control parameter were to be pressure of the magma chamber instead of Q_0, the above equations produce multiple equilibrium flows. In one case, a large flux of high volatile content low-viscosity magma would erupt; in the other a small flux of high-viscosity depleted magma would seep out.

Typical oscillations of elevation with time for a laboratory experiment like that sketched in Fig. 7(a) are shown in Fig. 8(a). The inferred phase plane of height–volume flux is shown in Fig. 8(b).

As mentioned in Sec. I, a large variety of physical systems have the behavior of these simple models.[18] Natural phenomena sometimes exhibit some of the features of these experiments such as abrupt transitions from one state to another or abrupt transitions to oscillations. In our case, the only difference between the steady and oscillating examples is the control parameter used in the physical system. We hope these simple demonstrations will lead to a clearer understanding of yet more important systems in the future.

ACKNOWLEDGMENTS

Thanks are due to Edward Spiegel for comments and advice. Support for WGL was from a summer student fellowship at Woods Hole Oceanographic Institution. The Physical Oceanography Program of the National Science Foundation, Ocean Sciences Division under Grant Nos. OCE-9633063 and OCE-0081179 supported the laboratory work.

[a]Electronic mail: jwhitchead@whoi.edu

[1]H. Stommel, ''Thermohaline convection with two stable regimes of flow,'' Tellus **13**, 224–230 (1961).

[2]J. Marotzke ''Ocean Models in Climate Problems,'' in *Ocean Processes in Climate Dynamics: Global and Mediterranean Examples*, edited by P. Malanotte-Rizzole and A. R. Robinson (Kluwer, Dordrecht, 1994), pp. 79–109; J. A. Whitehead, ''Thermohaline Ocean Processes and Models,'' Annu. Rev. Fluid Mech. **27**, 89–114 (1995).

[3]H. Stommel and Claes Rooth, ''On the interaction of gravitational and dynamic forcing in simple circulation models,'' Deep-Sea Res. **15**, 165–170 (1968).

[4]G. R. Ierley and V. A. Sheremet, ''Multiple solutions and advection-dominated flows in the wind-driven circulation. 1. Slip,'' J. Mar. Res. **53**, 703–733 (1995); Shi Jiang, Fei-Fei Jin, and Michael Ghil, ''Multiple equilibria, periodic, and aperiodic solutions in a wind-driven, double-gyre, shallow-water model,'' J. Phys. Oceanogr. **25**, 764–786 (1995).

[5]M. E. McCartney, ''Is the Ocean at the Helm?,'' Nature (London) **388**, 521–522 (1997); Ruth G. Curry, Michael S. McCartney, and Terrence M. Joyce, ''Oceanic Transport of Subpolar Climate Signals to Mid-depth Subtropical Waters,'' *ibid.* **391**, 575–577 (1998).

[6]J. A. Whitehead and Roger F. Gans, ''A new, theoretically tractable earthquake model,'' Geophys. J. R. Astron. Soc. **39**, 11–28 (1974).

[7]W. F. Budd, ''A first simple model for periodically self-surging Glaciers,'' J. Glaciol. **14**, 3–21 (1975).

[8]J. A. Whitehead and K. R. Helfrich, ''Instability of flow with temperature-dependent viscosity: A model of magma dynamics,'' J. Geophys. Res. B **96**, 4145–4155 (1991); Jonathan J. Wylie, Barry Voight, and J. A. Whitehead, ''Instability of magma flow from volatile-dependent viscosity,'' Science **285**, 1883–1885 (1999).

[9]F. H. Busse, ''Non-stationary finite amplitude convection,'' J. Fluid Mech. **28**, 223–239 (1967); D. Coles, ''Transition in circular Couette flow,'' *ibid.* **21**, 385–425 (1965); J. T. Stuart, ''Nonlinear Stability Theory,'' Annu. Rev. Fluid Mech. **3**, 347–370 (1971).

[10]P. Bernardet, F. Butet, M. Deque, M. Ghil, and R. L. Pfeffer, ''Low-frequency Oscillations in a Rotating Annulus with Topography,'' J. Atmos. Sci. **47**, 3023–3043 (1990); Eric R. Weeks, Yudong Tian, J. S. Urbach, Kayo Ide, Harry L. Swinney, and Michael Ghil, ''Transitions Between Blocked and Zonal Flows in a Rotating Annulus with Topography,'' Science **278**, 1598–1601 (1997).

[11]J. A. Whitehead, ''Multiple States in doubly-driven flow,'' Physica D **97**, 311–321 (1996); ''Multiple T–S States for Estuaries, Shelves and Marginal Seas,'' Estuaries **21**, 278–290 (1998)

[12]D. W. Oppo, J. F. McManus, and J. L. Cullen, ''Abrupt Climate Events 500,000 to 340,000 Years Ago: Evidence from Subpolar North Atlantic Sediments,'' Science **279**, 1335–1338 (1998); W. S. Broecker and G. H. Denton, ''The role of ocean-atmosphere reorganizations in glacial cycles,'' Geochim. Cosmochim. Acta **53**, 2465.2501 (1989).

[13]Esther M. Conwell, ''Negative Differential Conductivity,'' Phys. Today **23** (6), 35–41 (1970).

[14]Thomas L. Saaty and Joseph Bram, *Nonlinear Mathematics* (McGraw–Hill, New York, 1964), 381 pp.

[15]Francis Weston Sears and Mark W. Zemansky, *University Physics, Mechanics, Heat and Sound* (Addison–Wesley, Reading, MA, 1957), 2nd ed., pp. 240–242.

[16]Sir Horace Lamb, *Hydrodynamics* (1st American edition, Dover, New York, 1945), 6th ed., p. 21.

[17]R. M. Sutton, *Demonstration Experiments in Physics* (McGraw–Hill, New York, 1938), p. 110.

[18]H. Rouse, *Fluid Mechanics for Hydraulic Engineers* (Dover, New York, 1961), Eq. (222).

HEADED FOR GRIEF

Szilard had known what the neutrons would mean since the day he crossed the street in Bloomsbury: the shape of things to come. ''That night,'' he recalled later, ''there was very little doubt in my mind that the world was headed for grief.''

Richard Rhodes, *The Making of the Atomic Bomb* (Simon & Schuster, New York, 1986), p. 292.